International Journal of Hydrogen Energy 79 (2024) 164–176

Contents lists available at ScienceDirect

International Journal of Hydrogen Energy

journal homepage: www.elsevier.com/locate/he

Hydrogen storage integrated in off-grid power systems: a case study

Roberta Tatti [a], Mario Petrollese [a,*], Marialaura Lucariello [b], Fabio Serra [b], Giorgio Cau [a]

[a] Department of Mechanical, Chemical and Material Engineering, University of Cagliari, Cagliari, Italy
[b] Piattaforma Energie Rinnovabili, Sardegna Ricerche, Z.I. Macchiareddu, Uta, 09010, Cagliari, Italy

ARTICLE INFO

Handling Editor: Ibrahim Dincer

Keywords:
Green hydrogen
Hydrogen storage system
Off-grid energy system
Energy management strategy
Renewable energy
Parametric analysis

ABSTRACT

This paper investigates the feasibility and benefits of integrating hydrogen storage systems into off-grid power systems. As a case study, a stand-alone microgrid located on a small island in southeastern Sardinia (Italy) and already equipped with a photovoltaic (PV) system coupled with batteries is chosen.

To evaluate the integration benefits of the two storage systems (hydrogen and batteries) and the optimal sizing of the hydrogen storage section, a parametric analysis with a simulation model implemented in the MATLAB environment has been carried out. Results show that the optimal integration between the two storage systems is found by imposing a share of the batteries (18 kWh, 50% of the overall battery capacity) to exclusively supply the load demand (called battery energy buffer). In these conditions, an almost 100% self-sufficiency of the microgrid can be achieved by a hydrogen generator with the lowest size considered (2.4 kW), a hydrogen storage volume of 10 m^3 and a fuel cell, mainly able to completely cover the night loads, of 1.5 kW. This sizing leads to a Levelized Cost of Electricity (LCOE) for the hydrogen section of about 10.5 €/kWh.

Nomenclature

Symbols	
AA	Active Area [m^2]
c	Specific cost
E	Energy [Wh]
F	Total fuel cost [€]
f	Derating Factor [−]
GI	Global Irradiance [W/m^2]
HHV	Higher Heating Value [J/kg]
IR	Interest Rate [%]
$\dot{m}$	Mass Flow Rate [kg/s]
MM	Molar Mass [kg/kmol]
OM	Operating and Maintenance costs [€]
p	Pressure [bar]
P	Electric Power [W]
R	Ideal gas constant [kJ/(/kmol K)]]
SOC	State Of Charge [−]
t	Time [h]
T	Temperature [°C]
TCI	Total Capital Investment [€]
U	Heat Transfer Coefficient [$W/m^2/K$]
V	Volume [m^3]
α	Absorptance Coefficient [−]
γ	Temperature Coefficient [−]

(*continued on next column*)

(*continued*)

Symbols	
η	Efficiency [−]
τ	Transmittance Coefficient [−]
Subscripts	
A	Ambient Conditions
B	Battery
BC	Battery Charge
BD	Battery Discharge
BOP	Balance of Plant
C	Cell
EC	Engineering Cost
H_2	Hydrogen
INV	Inverter
L	Load
L,C	Load Curtailed
MOD	PV Module
NOCT	Nominal Operating Cell Temp.
NOM	Nominal Conditions
PV,L	PV Lost Power
STC	Standard Test Conditions
TR	Transportation
y	Years
Acronyms	
BEB	Battery Energy Buffer

(*continued on next page*)

* Corresponding author.
E-mail addresses: roberta.tatti@unica.it (R. Tatti), mario.petrollese@unica.it (M. Petrollese), lucariello@sardegnaricerche.it (M. Lucariello), fabio.serra@sardegnaricerche.it (F. Serra), giorgio.cau@unica.it (G. Cau).

https://doi.org/10.1016/j.ijhydene.2024.06.308
Received 4 December 2023; Received in revised form 19 June 2024; Accepted 22 June 2024
Available online 5 July 2024

(*continued*)

Symbols	
BESS	Battery Energy Storage System
BHESS	Battery and Hydrogen ESS
DG	Diesel Generator
EMS	Energy Management Strategy
ES	Energy System
ESS	Energy Storage System
FC	Fuel Cell
GHG	Greenhouse Gases
GHI	Global Horizontal Irradiance
HESS	Hydrogen ESS
HG	Hydrogen Generator
HT	Hydrogen Tank
LCOE	Levelized Cost of Electricity
PEC	Purchase Equipment Cost
PV	Photovoltaic
RES	Renewable Energy Source
SA	Stand-Alone
SAES	Stand-Alone Energy System
SCR	Self-Consumption Rate
SSR	Self-Sufficiency Rate
UH	Utilization Hours
WT	Wind Turbine

1. Introduction

The use of green hydrogen as an energy vector is becoming increasingly relevant in off-grid energy systems based on Renewable Energy Sources (RES) thanks to its flexibility with respect to site topography [1], its medium and long-term storage capacity [2,3] and the absence of Greenhouse Gases (GHG) emissions, both during production and use [4–6]. Currently, most off-grid system configurations are based on the use of Diesel Generators (DG) [7–9]. However, these systems have the disadvantage of rising operating costs, due to both the increased fuel costs and its transport [10], in addition to the high environmental impact, being characterized by GHG emissions [11]. For these reasons, several projects for the development of RES-based microgrids in off-grid sites have recently been proposed and numerous studies have already been carried out on RES-based microgrids in small islands, involving hydrogen systems [12]. Numerous research initiatives, including EU-funded projects like REMOTE [13] and Green Hysland [14], underscore the growing interest and ongoing efforts in this field. In addition, the European Union with the "Clean energy vision to clean energy action" supports the use of clean energy sources in European islands [15,16]. Other similar projects interest different remote islands in Europe, for example Canary Islands in Spain [17,18] and Orkney Islands in Scotland [19], and globally, for example the Thai islands (Thailand) [20]. In recent years, the development of reliable and sustainable energy solutions for off-grid systems has garnered significant attention also in the literature. Table 1 reports some studies concerning off-grid applications (distinguishing between islands and Stand-Alone, SA, areas), based on the coupling between an energy production source and an Energy Storage System (ESS), which could be a Battery ESS (BESS), a Hydrogen ESS (HESS) or an integrated Battery and Hydrogen ESS (BHESS).

The integration of an ESS, whether it is BESS, HESS or BHESS, into a RES-based microgrid follows a power-to-power path. Specifically, for the HESS, the electrical overproduction from RES-based systems, such as Photovoltaic (PV) systems or Wind Turbines (WT), is used to power a Hydrogen Generator (HG) [40], with an efficiency between 50% and 90%, depending on the size and type of the electrolyzer considered [41,42]. The hydrogen produced is then stored in Hydrogen Tanks (HTs) [43,44] characterized by a given storage capacity (according to different time scales, so hourly, daily or seasonal) at the production pressure or after compression at 350–700 bar [45]. The latter solution is mainly used in stationary applications, to increase the storage section energy density [46,47]. When RES-based systems are not able to satisfy the user needs, the stored hydrogen is used to produce electricity through a Fuel Cell (FC) [48,49].

Table 1
Studies on RES-based microgrids.

Author	PV	WT	DG	BESS	HESS	BHESS	Location
Gandiglio et al. [1]	✓		✓			✓	Island
Marocco et al. [21]	✓	✓		✓	✓	✓	Island
Marocco et al. [22]	✓			✓	✓	✓	Island
Nagasawa et al. [23]	✓	✓	✓	✓			Island
Fukaume et al. [24]	✓	✓			✓		Island
Gracia et al. [25]	✓		✓	✓		✓	Island & SA site
Zhang X. et al. [26]	✓	✓		✓		✓	Island
Kalinci et al. [27]	✓	✓			✓		Island
Østergaard et al. [28]	✓			✓			Island
Dawood et al. [29]	✓		✓	✓	✓	✓	SA site
Khiareddine et al. [30]	✓	✓		✓		✓	SA site
Castañeda et al. [31]	✓			✓	✓	✓	SA site
Nordin et al. [32]	✓			✓		✓	SA site
Zhang W. et al. [33]	✓	✓		✓	✓		SA site
Mulenga et al. [34]	✓		✓	✓			SA site
Mamaghani et al. [35]	✓	✓	✓				SA site
Das et al. [36]	✓	✓	✓	✓			SA site
Ameri et al. [37]	✓	✓	✓	✓	✓		SA site
Trapani et al. [38]	✓	✓	✓	✓		✓	Island
Hasan et al. [39]	✓	✓	✓		✓		Island
This Study	✓			✓		✓	Island

The importance of coupling a RES-based microgrid with an ESS is given by overcoming the limits due to the uncertainty of the primary energy source (i.e., sun, wind, etc.), which are non-dispatchable sources [50–52] and, thus, unable to meet instantaneous load demand when installed alone [53–55]. Batteries can be part of the ESS for short-term storage, as they offer high round-trip efficiencies and fast response times [56,57]. However, they are extremely sensitive to high temperatures and suffer from high self-discharge rates and lifetime uncertainty, making them unsuitable for long-term storage [58,59]. The still higher component costs and the relatively low roundtrip efficiency make HESS not yet competitive with mature storage systems currently used in on-grid applications, such as batteries [60]. On the other hand, hydrogen storage technologies have a longer useful life [61], better tolerance to high temperatures, and limited self-discharging effects [62,63]. For this reason, by integrating RES-based generators with both a battery bank and a hydrogen storage system, it is possible to reduce the electricity generation costs in off-grid sites [29,64]. In addition, the integration of a BHESS, if properly sized, can be cheaper than a RES-based microgrid only equipped with BESS [65].

To ensure that user needs are always satisfied, the definition of a proper Energy Management Strategy (EMS) is therefore necessary to establish the right priorities between the two different ESS [66–69]. Among the various management and control strategy models already implemented, Khiareddine et al. [30] modelled in MATLAB/Simulink an SA microgrid located in Tunisia (Sousse, Sahline region) according to six different scenarios: WT/BESS, WT/BHESS, PV/BESS, PV/BHESS, WT/PV/BESS and WT/PV/BHESS. The models proposed gave priority to batteries or hydrogen section with the aim of finding the best design for all technologies to cover the user loads. The results showed that the adoption of a BHESS could help reduce the need for a large and

expensive battery bank, despite the high investment cost of the HESS, thanks to the limited size required for the latter. Castañeda et al. [31] modelled in MATLAB an SA microgrid located in Álora (Spain), equipped with PV and coupled with a BESS, a HESS or a BHESS, respectively. Three energy management strategies were investigated for the proposed system configuration: the first is set to keep a certain load level of the batteries (40%), the second to maintain a certain level in both storages (40% and 20% for BESS and HESS respectively) and the latter is based on techno-economic strategies. The results showed that the batteries are used less in the third case, the use of HG and FC is minimized by implementing the first strategy, in which they reached the best energy efficiency, while the best energy efficiency considering the whole system was achieved in the second case. Nordin et al. [32] focused their studies on the analysis and modelling of an SA microgrid located in Johor Bahru, Malaysia, characterized by a PV plant integrated with a BESS or a BHESS. In both cases, the energy storage priority was given to batteries, while hydrogen production was activated after the battery was fully charged. The results showed that the integration of the HESS reduces the PV size, but the storage capacity of BESS should increase. The higher cost of the system composed by PV and BHESS is justified by the selling of the hydrogen produced. Zhang W. et al. [33] investigated the performance of an SA microgrid located in a remote area in Iran (Rafsanjan, Kerman), according to six scenarios: WT/HESS, PV/HESS, PV/WT/HESS, WT/BESS, PV/BESS and PV/WT/BESS. The results showed that with the HESS the best case is achieved by integrating PV and WT, while with the BESS the best case was obtained by the coupling of the sole WT.

By considering techno-economic analyses for assessing the energy production costs in off-grid conditions, Mulenga et al. [34] studied the techno-economic feasibility of a PV-DG system for rural electrification, located in Zambia. Three different load profiles (9%, 51% and 90% connection rate, respectively) and four different scenarios (DG, DG/PV, DG/PV/BESS and PV/BESS) were analyzed: the results showed that, despite the high capital cost of the PV/BESS scenario (the only one without DG), this is also the case with the lowest LCOE for the three load profiles. A similar study of a rural area was proposed by Mamaghani et al. [35], where the application of PV, WT and DG was analyzed for seven scenarios (DG, PV, WT, PV/WT, PV/DG, WT/DG and PV/WT/DG) in three different Colombian off-grid villages. In this case, the results for all areas demonstrated that the lowest LCOE is obtained for the PV/DG configuration. Moreover, Das et al. [36] proposed a techno-economic feasibility study focused on hybrid stand-alone systems, located in the five major cities of Bangladesh. For each city, five configurations were analyzed (DG, DG/PV/BESS, PV/WT/BESS/DG, PV/BESS and WT/BESS/DG), and the results showed that, for each area, the lowest LCOE is obtained for the PV/BESS/DG case, while the highest values are obtained for the case with the same components without the DG. Unlike previous studies, Ameri et al. [37] also considered energy production by hydrogen. The techno-economic analysis was carried out in four different locations in Cameroon, three load demand types and seven system configurations (PV/WT/BESS/DG, PV/BESS/DG, WT/BESS/DG, PV/WT/FC/DG, PV/FC/DG, WT/FC/DG, DG). The results showed that the lowest LCOE is reached with the PV/WT/BESS/DG configuration and high consumption, while the lowest costs are obtained for low consumption, considering the PV/FC/DG configuration.

The literature review concerning off-grid energy systems therefore demonstrates that the optimal configuration of an off-grid microgrid is not univocal but strongly depends on climatic and meteorological conditions of the site and load demand characteristics. In this regard, to the authors knowledge there are no studies relating to the analysis of off-grid systems characterized by strong seasonal variations in load demand, which typically occurs in small islands with peak loads during the warm periods [70]. From this point of view, the alternative system to the use of DGs should also include, alongside the RES-based production system, a storage system based on the combination of a short-term storage system coupled with a long-term one, such as a BHESS. On the other hand, a proper EMS should be developed to assure the right synergy among the two storage sections.

In this context, this paper aims to investigate the advantages of coupling a BHESS in a real microgrid powered by PV, located in a small island in southeastern Sardinia (Italy) and characterized by a large seasonal variation in the load demand. The current configuration of the RES-based microgrid includes a PV system and a BESS, while the benefits arising from the integration of a HESS are investigated in this paper. To evaluate the system performance and the yearly energy flows and to effectively scale the hydrogen storage system, a mathematical model has been developed in MATLAB and a proper EMS has been proposed. The main objectives of the study concerns:

- development of a control logic capable of guaranteeing the right coordination between the two storage systems (BESS for short-term storage and HESS for seasonal storage) to maximize the self-sufficiency of the system;
- development of an analysis methodology aiming at identifying the best sizing of the hydrogen storage section and battery bank capacity;
- the demonstration of the advantages of the integration of a BHESS compared to a BESS only system or the use of a diesel generator.

2. System configuration

The RES-based microgrid considered in this study is currently characterized by a PV system with a peak power of 7 kWp coupled with a 36 kWh battery bank. The installation of a HESS to be integrated with the BESS is planned in the near future to guarantee a self-sufficiency of the island as close as possible to 100% throughout the year. As shown in Fig. 1, the proposed configuration will ensure long-term storage, diversifying the supply of electricity from RES to users and therefore balancing the electrical loads of the microgrid.

The island utilities are mostly concentrated in the lighthouse and in the building where the HESS and the security, management and control systems will be installed. An estimation of energy consumption and the corresponding period in which the utilities will be used is reported in Table 2. As can be seen, important variations in the load demand are expected between the winter, when only the base loads should be satisfied, and the summer, characterized by the presence of tourists, research groups, etc., with a consequent increase in the electrical demand.

3. Mathematical models

The expected performance of the investigated RES-based microgrid in a typical year was evaluated through a mathematical model developed in MATLAB. Fig. 2 illustrates the method adopted to assess the expected system performance, carried out through the parametric analysis by varying the hydrogen section design (namely, the hydrogen generator and fuel cell sizes, the hydrogen tank volume) as well as the level of integration among BESS and HESS (controlled by the so-called battery energy buffer). These design variables are used as main input together with the yearly meteorological data and the defined load profiles for the determination of the hourly energy flows throughout the year. Each data is then processed by the Energy Management System, of which a detailed description is provided in section 3.4, to obtain the expected performance of the RES-based microgrid in terms of self-sufficiency rate (SSR), self-consumption rate (SCR), utilization time of the hydrogen section and levelized cost of electricity produced by the hydrogen storage section.

The meteorological data of the site under consideration was obtained using Meteonorm Software [71]. The user needs were modelled using a daily electrical load, according to the data reported in Table 2, for a typical summer day (considering the summer period between mid-June and mid-September) and a typical winter day (occurred in the rest of the

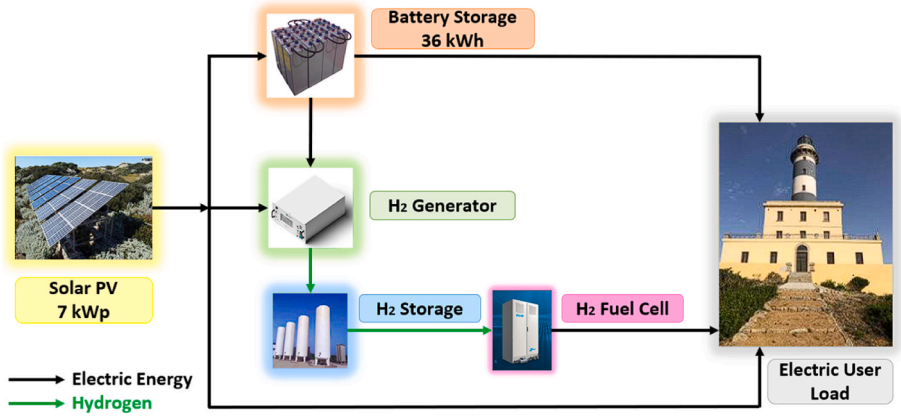

Fig. 1. Schematic of the RES-based microgrid analyzed.

Table 2
Utilities energy consumption.

Utilities	N	Winter load		Summer load	
		Power (kW)	Hour (h)	Power (kW)	Hour (h)
Video service	2	0.1	0–24	0.1	0–24
Smoke & Gas detector	3	0.13	0–24	0.13	0–24
Wireless	1	0.025	0–24	0.025	0–24
PC	12	–	–	0.05	10–18
Monitoring PC	1	0.05	0–24	0.05	0–24
Refrigerator	1	–	–	0.035	0–24
Air blower	1	0.025	0–24	0.025	0–24
Air Conditioning	1	–	–	0–1.45	10–18
Pump	1	–	–	0.5	18
Lighting	10	0.01	0–7 & 17–24	0.01	0–6 & 20–24
Water purifier	1	0.01	0–24	0.01	0–24
Other	–	–	–	0.2	0–24

year). Fig. 3 shows the two load profiles. As can be seen, an almost constant base load of 0.7–0.8 kW is requested in winter, while a large variation between base load (of about 0.9 kW) and peak load (of about 3 kW) occurs in summer, mainly due to the high consumption for air conditioning. The daily energy consumptions during winter and summer are 18.2 kWh/day and 38.85 kWh/day, respectively, for an expected annual consumption of 8.52 MWh/y.

In the following, the mathematical models implemented for evaluating the expected performance of each component of the considered RES-based microgrid will be described.

3.1. PV system

The PV generation profile was simulated starting from the data obtained by Meteonorm Software (as the ambient temperature, the diffuse and global horizontal irradiance, etc.) and the characteristics of the installed PV system. The latter is based on a 7 kWp PV plant, composed of modules characterized by a peak power of 250 Wp. Table 3 reports the main characteristics of the PV modules. Based on the current PV plant orientation, an azimuth angle of −30° and a tilt angle equal to 30° were considered.

The operating cell temperature T_C of the PV module was considered by taking the maximum between the ambient temperature, T_A, and the module cell temperature calculated, as reported in Equation (1):

$$T_C = \frac{T_A + \left(T_{NOCT} - T_{A,NOCT}\right)\frac{GI}{GI_{NOCT}}\frac{U_{PV,NOCT}}{U_{PV}}\left[1 - \eta_{PV,NOM}\frac{1-\gamma\left(T_{C,STC}+273{,}15\right)}{\tau\alpha}\right]}{1 + \left(T_{NOCT} - T_{A,NOCT}\right)\frac{GI}{GI_{NOCT}}\frac{\eta_{PV,NOM}\bullet\gamma}{\tau\alpha}} \tag{1}$$

where T_{NOCT} is the nominal operating cell temperature (NOCT, temperature of the cell without any load), with an incident radiation GI_{NOCT} of 800 W/m^2 and an ambient temperature $T_{A,NOCT}$ of 20 °C; GI is the

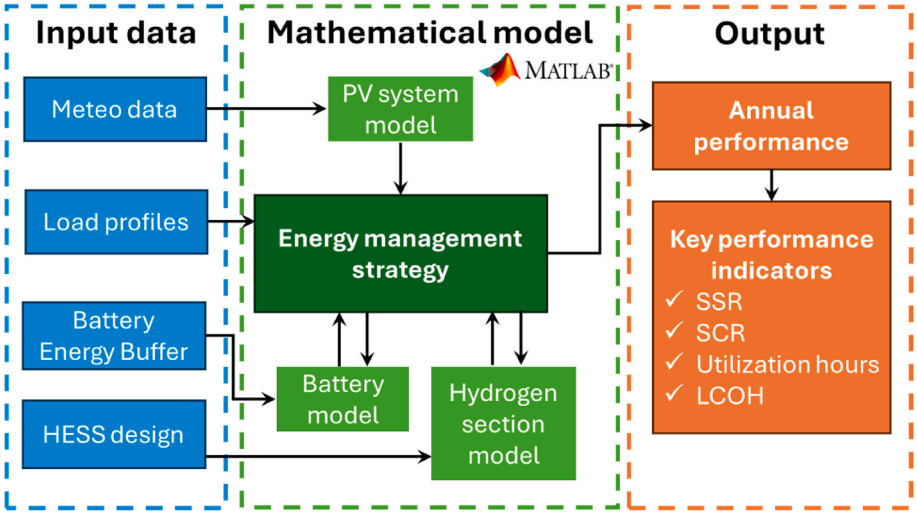

Fig. 2. Block diagram of the developed mathematical model.

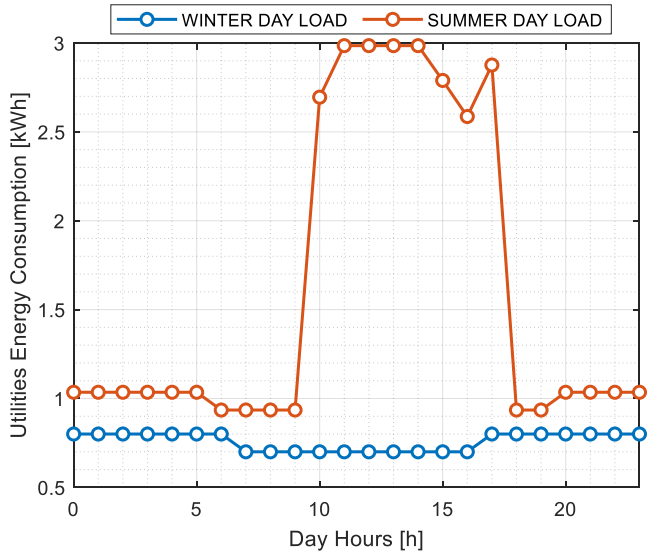

Fig. 3. Typical winter and summer load profiles.

Table 3
Key features of the PV module considered [72].

Parameter	Value
PV module power under Standard Test Conditions	250 W
PV net operative cell temperature (T_{NOCT})	45 °C
PV nominal efficiency ($\eta_{PV,NOM}$)	15.32%
PV Active Area (A_{MOD})	1.55 m^2
PV temperature coefficient (γ)	−0,486 %/°C
PV derating factor (f_{PV})	0.9
PV inverter efficiency (η_{INV})	90% ÷ 97.8%

global solar irradiation available on the surface of the PV array calculated through the Global Horizontal Irradiance (GHI) using the method proposed by Duffie et al. [73]; U_{PV} and $U_{PV,NOCT}$ are the heat transfer coefficients at the effective and NOCT conditions, respectively; $\eta_{PV,NOM}$ is the nominal PV efficiency, γ is the temperature coefficient, $T_{C,STC}$ is the PV cell temperature under standard test conditions (25 °C) and $\tau\alpha$ is the transmittance–absorption coefficient (assumed equal to 0.9). The actual PV efficiency η_{PV} was therefore obtained with Equation (2):

$$\eta_{PV} = \eta_{PV,NOM}\left[1+\gamma\left(T_C - T_{C,STC}\right)\right] \tag{2}$$

In particular, the power output P_{PV} of the PV subarray was calculated according to Equation (3):

$$P_{PV} = P_{PV,nom}\frac{GI}{GI_{NOCT}}\left[1+\gamma\left(T_C - T_{C,STC}\right)\right]\eta_{INV}\, f_{PV} \tag{3}$$

where η_{INV} is the inverter efficiency, given by the manufacturer as a function of the PV power output. Other secondary losses, like wiring losses, shading, soiling of the modules and aging are accounted in a derating factor f_{PV}. Based on the proposed model, the expected annual PV production is 10.17 MWh/year.

3.2. Battery storage

The energy stored in the battery bank was evaluated by determining its state-of-charge, SOC_B (Equation (4)), which indicates the ratio between the amount of stored energy and the nominal storage capacity.

$$SOC_B(t) = SOC_B(t-1) + \frac{\left(P_{BC}\,\eta_{BC} - \frac{P_{BD}}{\eta_{BD}}\right)\Delta t}{E_B} \tag{4}$$

where P_{BC} is the power input to the batteries (charging phase), P_{BD} is the power output to the batteries (discharging phase), η_{BC} and η_{BD} are the battery efficiency during charging and discharging phases, respectively (set both to 96% since the batteries are lead-acid type), Δt is the applied time step (equal to 1 h) and E_B is the battery nominal capacity. The battery depth-of-discharge was assumed equal to 70%.

3.3. Hydrogen section

The HESS includes a HG, which is powered in case of electrical overproduction during the day and if there is sufficient energy in the batteries during the night, storage tanks, in which hydrogen is stored at the production pressure for a postponed use, and a FC, which converts the hydrogen produced into electricity if it is not possible to satisfy the user needs with PV and/or batteries. Both the size of the HG and the capacity of storage tanks were considered design parameters to be varied during the parametric analysis.

Concerning the HG, a commercial electrolyzer based on the AEM technology and characterized by a modular stack with nominal power of 2.4 kW, with a hydrogen production of 0.5 Nm^3/h at 35 barg, was considered [74]. According to the manufacturer specification, it was assumed that the HG can operate in a range between 60% and 100% of its rated power. The system is scalable and the optimal number of stacks of the considered application is therefore chosen based on the results obtained by the parametric analysis. Since the PV power supplying the hydrogen section and the user needs are time dependent, the HG often operates in off-design mode with variable efficiency. Therefore, the hydrogen mass flow rate $\dot{m}_{H_2}$ produced by a given HG power supply P_{HG} depends on the electrolyzer efficiency η_{HG}, given by Equation (5) [75].

$$\eta_{HG} = \frac{\dot{m}_{H_2}\, HHV_{H_2}}{P_{HG}} \tag{5}$$

where HHV_{H_2} is the Higher Heating Value of the hydrogen.

To evaluate the variation of the HG efficiency with the power rate, the modelling of an AEM electrolyzer proposed by Gul et al. [76] was adopted. The main parameters, used for assessing the characteristic curve of the electrolyzer, are reported in Table 4. Fig. 4 shows the net efficiency of the HG (including the energy consumption of the auxiliary systems) implemented in the model.

On the other hand, the size of the FC was assumed constant and equal to about 3 kW to guarantee the supplying of the maximum load demand, even if PV and battery are not in operation. The fuel cell, based on PEM technology, is able to operate in a wider range, between about 20% and 100%. It was also assumed that the minimum pressure of hydrogen

Table 4
AEM hydrogen generator [76] and PEM fuel cell [77] parameters used in the model.

Hydrogen generator parameters	Value
Cell area	250 cm^2
Membrane thickness	0.005 cm
Membrane resistance	70 Ω cm^2
Contact resistance	0.00001 Ω cm^2
Anode charge transfer coefficient	0.2 A/cm^2
Cathode charge transfer coefficient	1 A/cm^2
Stack temperature	60 °C
Anode exchange current density	0.5 A/cm^2
Cathode exchange current density	0.7 A/cm^2
Fuel cell parameters	**Value**
Cell area	100 cm^2
Internal resistance	0.7 Ω cm^2
Amplification constant	0.085
Anode charge transfer coefficient	0.4 A/cm^2
Cathode charge transfer coefficient	0.4 A/cm^2
Stack temperature	50 °C
Exchange current density	$10^{-6.912}$ A/cm^2

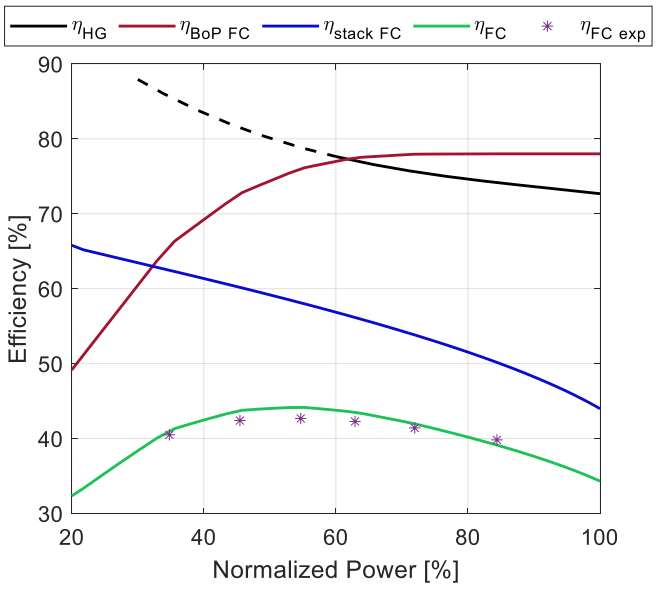

Fig. 4. Hydrogen generator and fuel cell efficiency as a function of load conditions.

feeding the FC must be at least 2 barg. As for the HG, also the FC often operates in off-design conditions with variable efficiency. The electrical power P_{FC} generated by the FC depends on the FC efficiency η_{FC}, according to Equation (6) [77].

$$\eta_{FC} = \frac{P_{FC}}{\dot{m}_{H_2} HHV_{H_2}} \tag{6}$$

In this case, the efficiency curve was obtained starting from the mathematical model proposed by Spiegel [78] and characterized by the parameters reported in Table 4.

Fig. 4 shows the FC net efficiency, given by the product of the stack efficiency and of the Balance of Plant efficiency. As depicted in the figure, the FC efficiency curve was finally validated with experimental data of a kW-scale fuel cell (indicated as markers in Fig. 4) provided by a FC manufacturer.

Finally, the energy stored inside the hydrogen storage system at a given time (t) was evaluated using the state-of-charge of the HT, SOC_{H_2}, determined by Equation (7), which allows to monitor the energy converted by the electrolyzer and that used by the FC.

$$SOC_{H_2}(t) = SOC_{H_2}(t-1) + \frac{\left(P_{HG}\,\eta_{HG} - \frac{P_{FC}}{\eta_{FC}}\right)\Delta t}{E_{H_2}} \tag{7}$$

The nominal hydrogen storage capacity (E_{H_2}) was calculated using Equation (8), based on the HHV of hydrogen (equal to 141.78 MJ/kg) and the nominal mass of hydrogen that can be stored in the hydrogen tanks, obtained by the ideal gas equation. In particular, the net pressure of the tanks (difference between the nominal pressure, p_{NOM}, of 35 barg, and the minimum hydrogen pressure required for the FC to start producing electricity, p_{min}, 2 barg), the nominal volume (V_{HT}, which varies during the parametric analysis), the ideal gas constant (R, equal to 8.314 kJ/kmolK), a temperature T of 25 °C and the molar mass of hydrogen (MM_{H_2}, 2.016 kg/kmol) were considered.

$$E_{H_2} = HHV \bullet \left[\frac{(p_{NOM} - p_{min}) \bullet V_{HT} \bullet MM_{H_2}}{R \bullet T}\right] \tag{8}$$

3.4. Energy management strategy

A detailed EMS for the analyzed RES-based microgrid was implemented in MATLAB, with the aim of maximizing both the self-sufficiency of the microgrid, thus minimizing the periods when the load demand is not satisfied, and the Utilization Hours (UH) of the hydrogen storage system. For this reason, the energy stored in batteries was divided into two distinct parts: a share of the battery capacity, called Battery Energy Buffer (BEB) is exclusively used to feed the load demand, while the remaining part can be used both for covering the user needs and to partially support the hydrogen production, even during the night, with the aim of increasing the utilization hours of the hydrogen storage system. Based on this approach, the implemented EMS is shown as logical diagram in Fig. 5. Obviously, user needs always have the priority on the charging of the ESS. In case the PV production exceeds the load demand, the energy surplus is used to produce hydrogen until the HT is not fully charged. If the energy surplus is lower than the minimum HG load, the hydrogen production is supported by the share of the battery capacity, not involved in the BEB. Batteries are therefore charged in case of PV overproduction when the HG is already turned on at the maximum power or if it is not possible to feed it at the minimum power.

During deficit periods, user needs are satisfied primarily with the energy stored in the BEB. If this stored energy is not sufficient, the FC operates to cover the load demand. The HG is turned on when the energy stored in batteries not involved in the BEB is sufficient to feed it at least at the minimum power, while batteries will be charged if user needs will be less than the sum of PV and FC production.

3.5. Key performance indicators

The analysis of yearly energy performance of the proposed RES-based microgrid is based on two key performance parameters: the Self-Sufficiency Rate (SSR) and the Self-Consumption Rate (SCR), which give an indication of the ability to satisfy the user needs and to use all the electricity production, respectively. Specifically, the SSR and the SCR were evaluated based on Equation (9) and Equation (10), respectively:

$$SSR = \frac{E_L - E_{L,C}}{E_L} \tag{9}$$

$$SCR = \frac{E_{PV} - E_{PV,L}}{E_{PV}} \tag{10}$$

where E_L and E_{PV} are the annual energy requested by the user and produced by PV, respectively, $E_{L,C}$ is the annual load curtailed, i.e., the amount of load request that cannot be satisfied, and $E_{PV,L}$ is the share of annual PV overproduction that cannot be stored since the two storage systems are fully charged and, thus, it is lost.

Together with these two parameters, the utilization hours of the HG and FC, that are the overall period the two hydrogen-based systems are in operation, are analyzed in detail.

A preliminary economic analysis of the RES-based microgrid was finally carried out by calculating the Levelized Cost of Electricity produced by the sole hydrogen storage section ($LCOE_{H_2}$), as reported in Equation (11):

$$LCOE_{H_2} = \frac{TCI + (OM \bullet TCI) \bullet \sum (1+IR)^{-y}}{E_{FC} \bullet \sum (1+IR)^{-y}} \tag{11}$$

where TCI is the Total Capital Investment, OM is the percentage of Operating and Maintenance costs related to TCI, E_{FC} is the annual energy produced by the FC, IR is the Interest Rate and y is the total number of years. In particular, the TCI was calculated by means of Equation (12) starting from the Purchase Equipment Costs (PEC), as a function of the size of the hydrogen section components and their specific costs, listed in Table 5.

$$TCI = \left[\left(c_{HG}P_{HG,nom} + c_{HT}V_{HT} + c_{FC}P_{FC,nom}\right)(1 + c_{BOP})\right](1 + c_{EC}) \tag{12}$$

where c_{BOP} are the costs for the balance of plant (expressed as a percentage of the PEC) and c_{EC} are the Engineering Costs (expressed as a

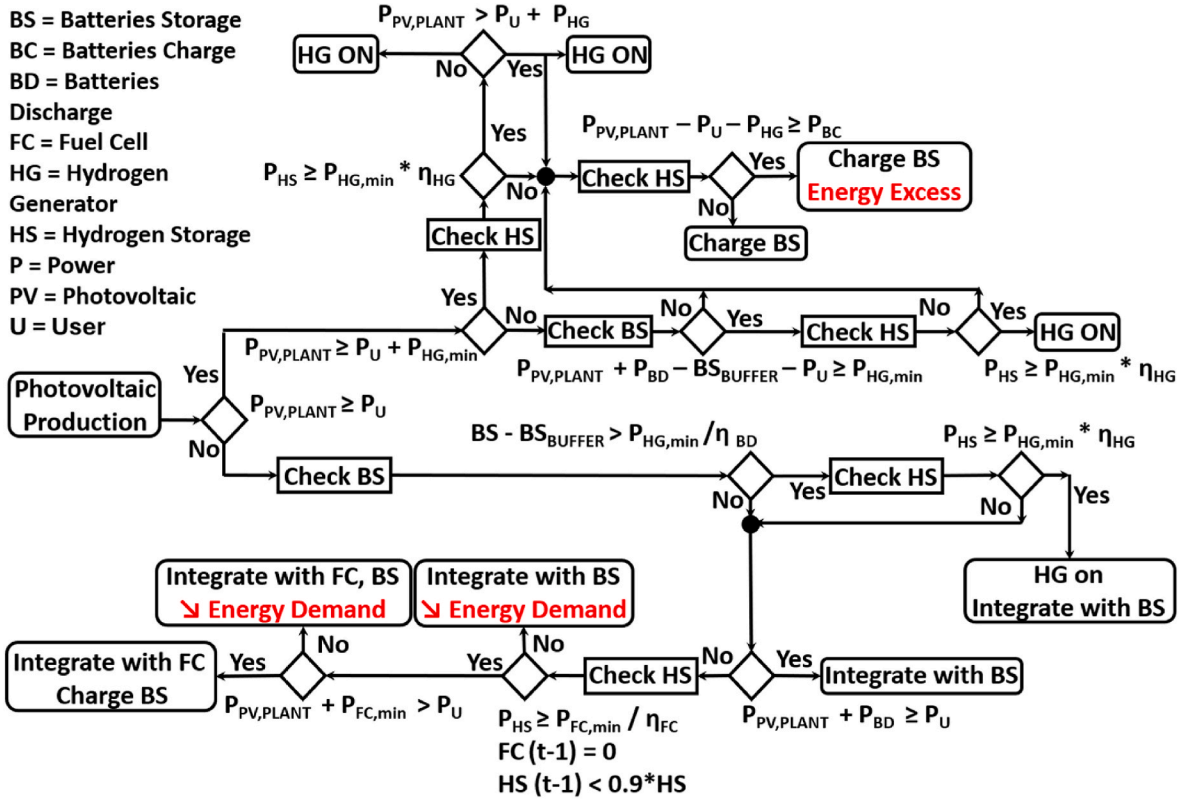

Fig. 5. Energy management strategy.

Table 5
Main parameters assumed for the preliminary economic analysis.

Parameter	Value
Operating and Maintenance costs (*OM*) [79]	5% of the TCI
Interest Rate (*IR*) [79]	5%
Lifetime (*y*) [79]	20 years
Balance of Plant costs (c_{BOP}) [79]	10% of the PEC
Engineering costs (c_{EC}) [79]	10% of PEC+BOP
Hydrogen generator specific costs (c_{HG}) [80]	$3165.72\ (P_{HG,nom})^{0.885}$
Hydrogen tank @35 bar specific costs (c_{HT}) [80]	83.69 €/m^3
Fuel cell specific costs (c_{FC}) [4]	2500 €/kW

percentage of the PEC + BOP costs).

In order to make a comparison between the costs related to the energy production using hydrogen ($LCOE_{H_2}$) and the economic expense due to the integration of a DG, the LCOE of the energy produced by the DG was calculated by means of Equation (13).

$$LCOE_{DG} = \frac{TCI_{DG} + [OM \bullet TCI_{DG} + F \bullet (1 + c_{TR})] \bullet \sum (1 + IR)^{-y}}{E_{DG} \bullet \sum (1 + IR)^{-y}} \quad (13)$$

Equation (13) is similar to Equation (11), in which the TCI_{DG} is calculated in the same way reported in Equation (12), with PEC characterized by the only DG capital cost (assumed equal to 1500 €/kW), while *F* is the total fuel cost, according to Equation (14), c_{TR} is the cost for fuel transportation (10% of *F*) and E_{DG} is the annual energy produced by DG.

$$F = \left[\sum_{1}^{8760} A \bullet P_{DG}(t) + B \bullet P_{DG,nom} \right] \bullet c_F \quad (14)$$

In Equation (14), P_{DG} is the power produced by DG at time *t*, $P_{DG,nom}$ is the nominal power of DG (assumed equal to the peak load, i.e. 3 kW), *A* and *B* are consumption curve coefficients, assumed equal to 0.246 l/kWh and 0.0845 l/kWh respectively [37], and c_F is the specific fuel cost, assumed equal to 1.87 €/l.

4. Results and discussion

In this section, the expected annual performance of the RES-based microgrid is shown and the main outcomes are discussed. The key performance indicators are evaluated for different sizing of the HESS section, in terms of hydrogen storage capacity and HG nominal power, and by varying the share of battery capacity dedicated to the BEB with the aim of finding the best integration for the two ESS (both the storage systems are considered completely discharged at the beginning of the year).

4.1. Annual performance of the RES-based microgrid

Starting with an electrolyzer module, a rise in the HT size from 3 m^3 to 15 m^3 and the variation of the BEB size between 0% ÷ 100% of the nominal battery capacity is analyzed and their effect on the microgrid performance is shown in Fig. 6. As can be observed, there are two contrasting effects in choosing the BEB size. Setting the buffer equal to zero (BEB=0) means placing the batteries at the service of the HESS: in this way all the energy produced is consumed (SCR=1, Fig. 6(b)), but this quantity is not sufficient to cover the user needs (SSR<0.7, Fig. 6 (a)). Looking at the yearly utilization hours of HG and FC (Fig. 6(c) and (d), respectively), the HESS is frequently in operation, with utilization hours for the HG and FC that reach their maximum value. However, since the hydrogen storage system is characterized by a lower round-trip efficiency compared to batteries, a significant reduction in the average system efficiency occurs, resulting in a deficit in the complete supply of the load requests. On the other hand, the use of batteries exclusively to feed the user needs (BEB≥28.8 kWh) does not allow the HESS to operate adequately (the utilization hours for the HG and the FC are zero) and, consequently, the only use of batteries cannot compensate for the mismatch between energy production and demand (SSR<0.94), while

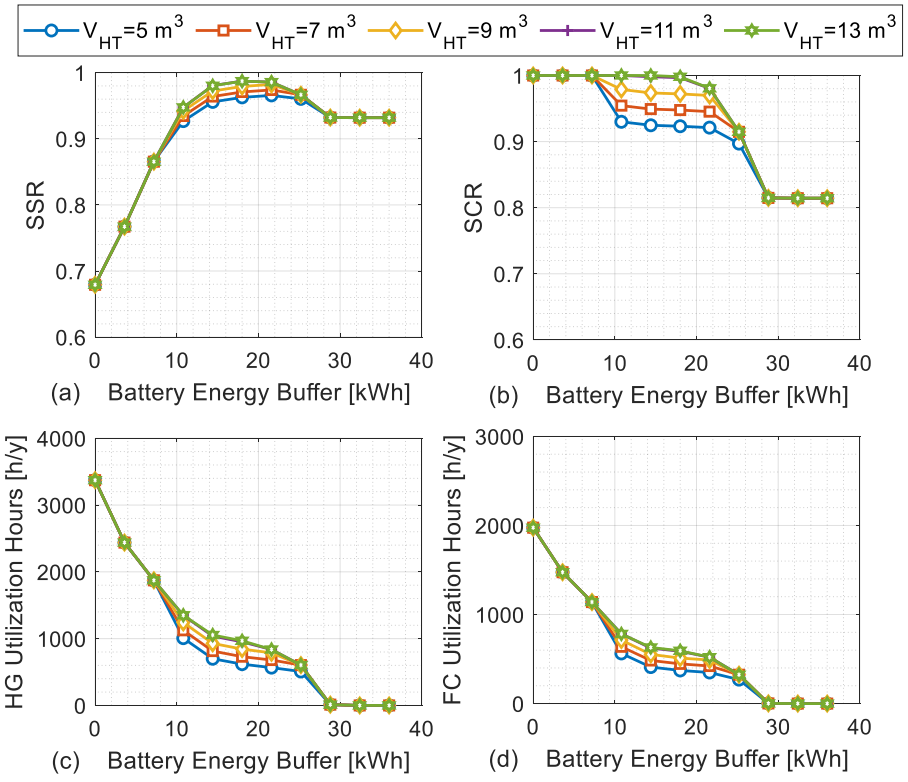

Fig. 6. Annual performance of the RES-based microgrid with a hydrogen generator of 2.4 kW.

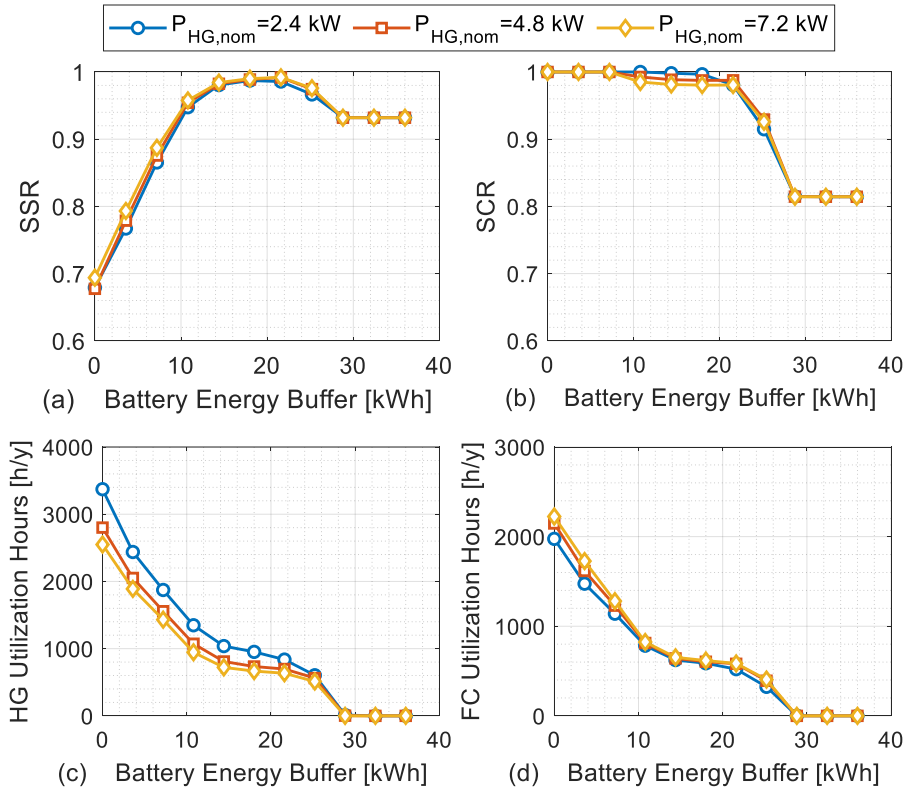

Fig. 7. Annual performance of the RES-based microgrid with a hydrogen tank volume of 9 m^3.

there is a large amount of energy produced by PV that is not used nor stored (SCR<0.82). The best results are therefore obtained for a BEB set between 50% and 60% (18 kWh and 21.6 kWh respectively), where SSR values close to 99% can be achieved, with the highest value (SSR=98.7%) obtained for a 50% BEB (18 kWh). In this interval, the effect of the HT size on the system performance is not negligible up to storage volumes lower than 11 m^3, while a very marginal improvement occurs with a further increase of the storage capacity. As increasing the HT size would mean an increase of the HESS costs, the HT size should be chosen equal to the lowest size, i.e. 11 m^3, which corresponds to a hydrogen storage capacity of about 980 kWh.

With this design choice, the increase of the HG size as a function of the BEB is analyzed (Fig. 7). Particularly, as the HG selected is scalable, the variation in the HG power from 1 to 3 modules, so between 2.4 kW and 7.2 kW, is investigated. As can be seen in Fig. 7(a), the HG size has not a relevant influence on the SSR, since only marginal variations are observed for low values of BEB. A similar trend also characterizes the SCR (Fig. 7(b)) and the FC Utilization Hours (Fig. 7(d)). Conversely, as highlighted in Fig. 7(c), the size of HG strongly influences the utilization hours of this component: for the same amount of annual energy supplied, in fact, the HG with the lowest size would run more compared to the case with 3 modules (952 h/y instead of 666 h/y, by considering a BEB=50%). Since the rise in the HG nominal power does not lead to any energy benefits but has a negative impact on the cost-effectiveness of the hydrogen storage section due to the high capital costs and the lower utilization factors, a 2.4 kW HG appears to be the optimal option. Looking at the overall utilization time of the hydrogen section (Fig. 7(c) and (d)), this is a little bigger for BEB=50% in comparison with the case of a BEB of the 60% (1539 h/y against 1358 h/y). Also, considering the previous results, a BEB of 50% (18 kWh) was chosen.

To verify if the optimal sizing of the hydrogen components deriving from the energy analysis is also acceptable from an economic point of view, the Levelized Cost of Electricity was calculated by varying the hydrogen storage volume and HG nominal power, by keeping the FC nominal power and the battery energy buffer set equal to 3 kW and 18 kWh, respectively. As shown in Fig. 8, the minimum $LCOE_{H_2}$ is achieved, as expected, for the HG with the lowest size, while the hydrogen storage size that guarantees the lowest $LCOE_{H_2}$, equal to 12.83 €/kWh, is 11 m^3. These results confirm that the hydrogen component's size chosen in the yearly performance analysis was well suited from a techno-economic point of view.

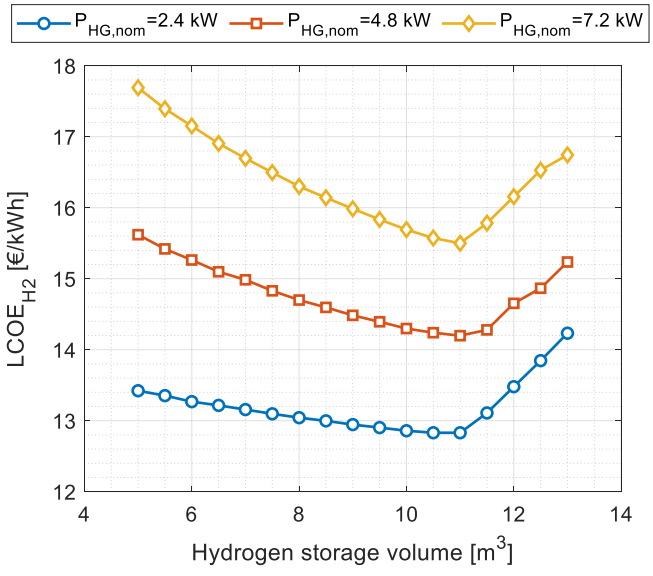

Fig. 8. Levelized cost of electricity produced by the hydrogen section as a function of hydrogen storage volume and hydrogen generator size.

With this BHESS size configuration (2.4 kW HG, 11 m^3 HT, 3 kW FC and 18 kWh BEB), the annual filling trend of the two ESSs has been analyzed: the results are shown in Fig. 9, in which the vertical dotted red lines indicate the summer period, between mid-June and mid-September. As can be observed in the trend of the HT energy stored over time (Fig. 9(a)), the first part of the year could be divided in other two periods: a first sub-period up to the 1800 h of the year, and a subsequent one up to the beginning of summer. The first sub-period is characterized by a low utilization of hydrogen technologies, due to the low energy available for the electrolyzer, unable to turn on at its minimum power, and the consequent low level of stored hydrogen available for the FC. The second sub-period is, instead, mainly characterized by the production of hydrogen, thanks to the growing amount of electricity produced by the PV plant, which allows not only to cover the loads but also to frequently turn-on the hydrogen generator. During this period, a continuous rise in the hydrogen storage level can be therefore observed (the energy deficit occurred during the night is mainly covered by batteries), reaching the full charge of the HT (about 1000 kWh) at the mid-June. In summer, although the high PV energy production, an energy deficit often occurs and both ESSs are used to cover the load demand. Consequently, a continuous decrease of the stored hydrogen occurs, due to the large use of the FC, while the average state-of-charge of the batteries is strongly reduced, as can be observed in Fig. 9(b). The last period of the year is characterized by both hydrogen production, thanks also to the support of the batteries, and hydrogen consumption, when the BESS is almost completely discharged. This figure therefore demonstrates the diversified role of the two storage systems given by the implemented EMS: the HESS is used mainly as a seasonal storage system, as HG is used mostly in the spring while FC in the summer, and the BESS is used as a short-term storage, especially during the summer, when the PV production and the user demand are greater.

Finally, the utilization of the hydrogen storage system has been analyzed and the total yearly number of HG and FC utilization hours at a given power is shown in Fig. 10.

Regarding the HG (Fig. 10(a)), it operates in a total of 952 h/year, of which 631 h/year (66.28%) close or equal to its nominal power (2.4 kW). For this reason, the HG could be considered correctly sized. Looking at the FC utilization (Fig. 10(b)), it is used with a power equal to or lower than 1.1 kW for 579 h (98.64%) and only for 8 h (1.36%) with a higher power. This happens because the FC is not used as a main energy source to cover the summer peak loads during the daytime, mainly satisfied by the PV and batteries, but it almost always operates at night, when the batteries are at minimum capacity (i.e. SOC_B=30%), to cover base loads.

4.2. Sensitivity analysis on fuel cell power

Given the oversizing of the FC nominal power, further analysis was conducted to assess the expected annual performance by varying the FC size from 0.5 kW to 3 kW. The results obtained in terms of SSR and FC

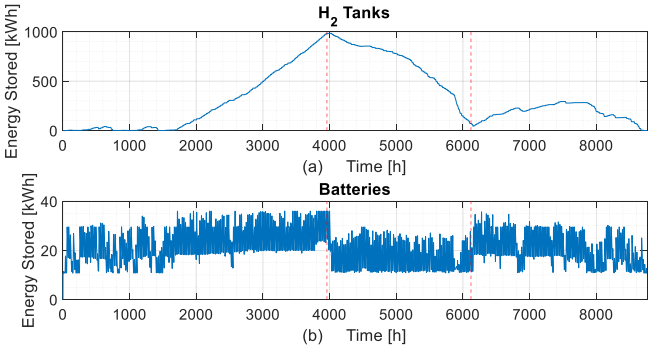

Fig. 9. Energy stored in (a) hydrogen tanks and (b) batteries over time.

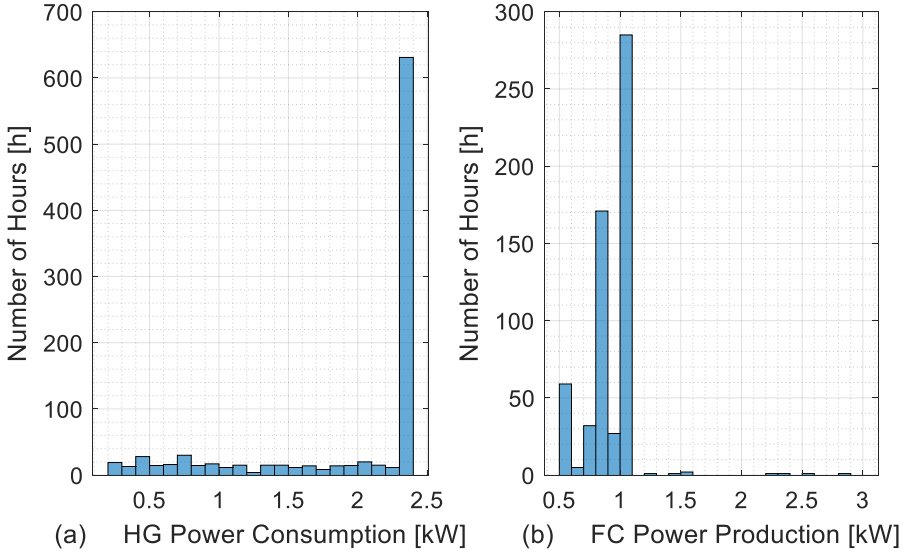

Fig. 10. Operating conditions of the (a) hydrogen generator and (b) fuel cell during the year.

utilization hours are shown in Fig. 11 (both SCR and HG utilization hours do not vary with the FC size). As illustrated, the SSR (Fig. 11(a)) exceeds 99% for FC sizes between 1.2 kW and 2.5 kW alongside hydrogen tank volumes exceeding 10 m^3. This trend strongly depends on the minimum night load request, equal to 0.7 kW and 1.035 kW during the winter and summer, respectively. Consequently, for a FC size lower than 1 kW the additional use of batteries is requested to completely cover the user demand during the night, but this storage section is often not sufficient to completely meet this need. Conversely, an FC with a nominal power close to 3 kW experiences frequent operation at minimum load, leading to a decrease in average conversion efficiency.

To find the best size of FC and of the hydrogen tank, the $LCOE_{H2}$ was assessed, considering variations in FC size and hydrogen tank volume while maintaining the HG rated power constant at 2.4 kW and the battery energy buffer at 50% (18 kWh). As shown in Fig. 11(b), the curves related to a hydrogen storage equal or lower than 10 m^3 reach a minimum value close to a FC size equal to 1.5 kW, while for a higher hydrogen storage the minimum is reached for a FC nominal power of 1.2 kW. However, hydrogen storage values of 9 m^3 or lower fail to maximize the SSR, and despite the lowest costs, these storage sizes are not acceptable from an energy point of view. Therefore, the best compromise between maximizing self-sufficiency and minimizing electricity costs is found for a FC size of 1.5 kW and for a hydrogen tank volume of 10 m^3, where the $LCOE_{H_2}$ reaches its minimum value (10.50 €/kWh) and the SSR is higher than 99%. Finally, the optimal microgrid components sizes resulting from the parametric analysis are a 2.4 kW HG, a 10 m^3

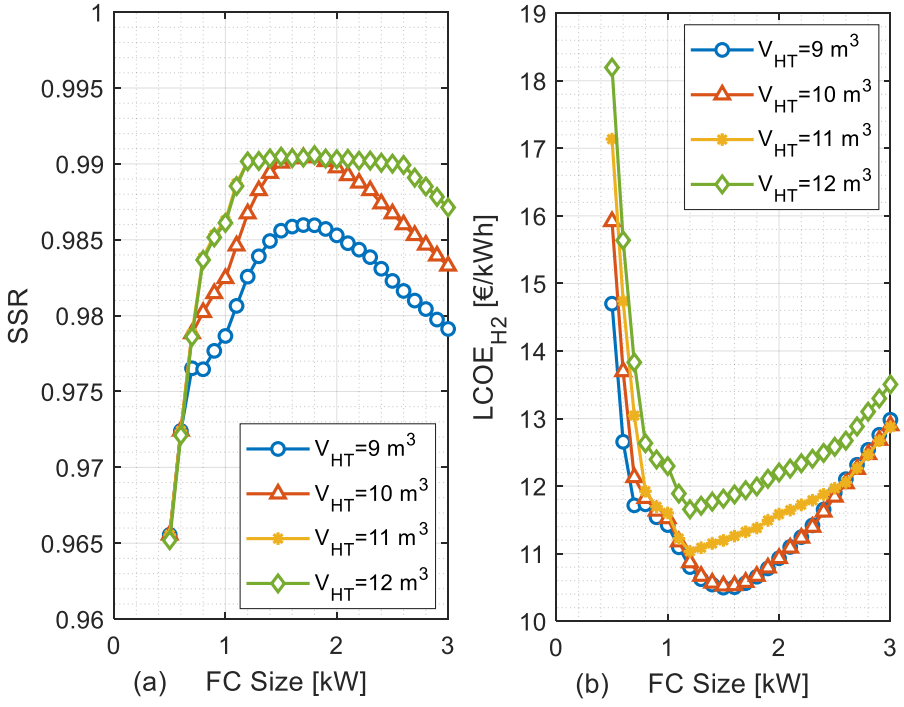

Fig. 11. Self-sufficiency Rate of the RES-based microgrid (a) and Levelized Cost of Electricity produced by the hydrogen section (b) as a function of fuel cell nominal power and hydrogen storage volume.

HT, a 50% BEB (18 kWh) and a 1.5 kW FC.

4.3. Comparison with the current microgrid configuration

In this section, the performance obtained by the RES-based microgrid equipped with the proposed BHESS are compared with those achieved by the current configuration, i.e., the PV system coupled with the BESS. As mentioned above, the total yearly PV production is equal to about 10 MWh/year, while the user need is about 8.5 MWh/year. With the only use of batteries as ESS, the achieved SSR and SCR are equal to 93.2% and 81.4%, respectively. This indicates that without the integration of a HESS a greater amount of user needs will not be satisfied (6.8% compared to only 1% with BHESS integration). Specifically, the energy deficit is equal to 579.8 kWh/y (distributed over 739 h/y), while with the BHESS it is only 83.82 kWh/y (distributed over 122 h/y). The periods during which the microgrid fails to cover load requests are illustrated in Fig. 12. With BHESS (Fig. 12(a)) the energy deficit primarily occurs in the winter period, while with BESS (Fig. 12(b)) load curtailment happens both in winter, approximately 222 kWh/y (distributed over 325 h/y), and summer, approximately 357 kWh/y (distributed over 414 h/y). In the case with BHESS, a solution could be lowering not essential loads during the winter, for example turning off some lights. In the case with BESS, characterized by a more relevant energy deficit, the days in which it is necessary to lower the loads should be more than double compared to the previous case to guarantee the same SSR during the winter. Furthermore, in the summer period there would still be a high energy deficit such as not to guarantee the supply of essential loads. This also underscores the fact that merely increasing the battery storage capacity may not be an effective solution since, due to the seasonality of load demand, significant PV overproductions occur in spring and autumn, necessitating a long-term storage system to shift large amounts of stored energy throughout the seasons.

To ensure the energy not produced by the system configuration equipped only with BESS, a diesel generator (DG) would need to be introduced, capable of producing at least 579 kWh/year to achieve an SSR close to 100 to assess the economic implications of integrating the DG, a preliminary economic analysis was carried out calculating the LCOE of the energy produced by the DG using Equation (13). Based on the assumptions outlined in Section 3.7, a $LCOE_{DG}$ of about 2 €/kWh was determined. The disparity between these costs reflect the additional expense incurred for ensuring 100% green electricity production without greenhouse gas (GHG) emissions. It is important to note that significant reductions in the capital costs for hydrogen technologies are expected in the next, which will likely lead to a considerable reduction in this price gap.

5. Conclusions

In this study, an energy assessment of a green hydrogen energy system used for seasonal storage in an off-grid small island in south-eastern Sardinia (Italy) was conducted. A mathematical model was developed using MATLAB and a parametric analysis was conducted to analyze the yearly performance of the RES-based microgrid for different sizes of the hydrogen storage section and various level of integration between hydrogen and battery sections.

The results revealed that with the current microgrid configuration, characterized by a PV system integrated with batteries, approximately 93% of user needs could be met, while about 580 kWh/year of the load request would need to be curtailed. With the integration of the hydrogen storage section in the current microgrid, a significant improvement in the system performance was achieved. Specifically, with a 2.4 kW HG, 1.5 kW FC, 10 m^3 HT (equivalent to a storage capacity of about 900 kWh) and 18 kWh BEB, the 99% of the annual load request can be satisfied, while the electricity deficit (equal to 83.82 kWh/y) occurs majorly during winter. Furthermore, the Levelized Cost of Electricity produced by hydrogen is close to 10.5 €/kWh. The trends obtained from

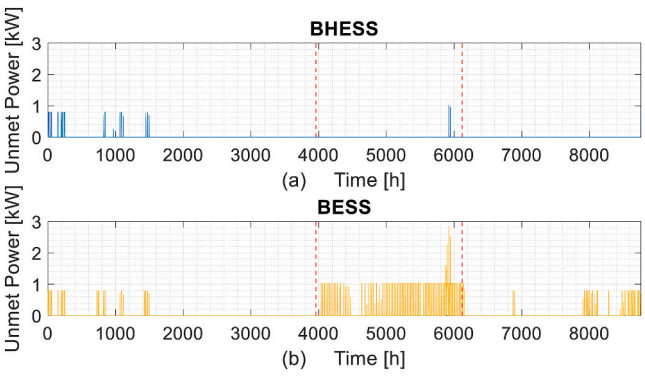

Fig. 12. Energy deficit with the integration of BHESS (a) and BESS (b).

the energy stored in the two energy storage systems during the year highlighted their different roles given by the proposed energy management strategy, with batteries primarily used as short-term storage, especially during summer, while the HESS served principally as seasonal storage. This underscores the validity of the proposed control strategy and of the method applied for sizing the hydrogen storage system, which can be extended to other similar cases characterised by important seasonal variation in the load demand. Finally, while the quantitative results obtained by a preliminary economic analysis are influenced by various factors and assumptions, they provide valuable insights into the additional costs associated with maintaining a 100% green energy supply on off-grid islands by using BHESS solution.

CRediT authorship contribution statement

Roberta Tatti: Writing – original draft, Methodology, Investigation, Conceptualization. **Mario Petrollese:** Writing – review & editing, Writing – original draft, Methodology, Formal analysis, Conceptualization. **Marialaura Lucariello:** Writing – review & editing, Validation, Formal analysis. **Fabio Serra:** Writing – review & editing, Visualization, Validation, Software. **Giorgio Cau:** Writing – review & editing, Supervision.

Declaration of competing interest

The authors declare that they have no known competing financial interests or personal relationships that could have appeared to influence the work reported in this paper.

Acknowledgments

This paper is a part of a research project carried out in the framework of a collaborative research agreement between Sardegna Ricerche, the Department of Mechanical, Chemical and Materials Engineering of the University of Cagliari, and H2D Energy S. r.l., for the development of the research project “Green Hyland”, in Sardinia.

References

[1] Gandiglio M, Marocco P, Bianco I, Lovera D, Blengini GA, Santarelli M. Life cycle assessment of a renewable energy system with hydrogen-battery storage for a remote off-grid community. Int J Hydrogen Energy 2022;47(77):32822–34. https://doi.org/10.1016/J.IJHYDENE.2022.07.199.

[2] Ceylan C, Devrim Y. Green hydrogen based off-grid and on-grid hybrid energy systems. Int J Hydrogen Energy 2023;48(99):39084–96. https://doi.org/10.1016/J.IJHYDENE.2023.02.031.

[3] Argyrou MC, Christodoulides P, Kalogirou SA. Energy storage for electricity generation and related processes: technologies appraisal and grid scale applications. Renew Sustain Energy Rev 2018;94:804–21. https://doi.org/10.1016/J.RSER.2018.06.044.

[4] Abdin Z, al Khafaf N, McGrath B. Feasibility of hydrogen hybrid energy systems for sustainable on- and off-grid integration: an Australian REZs case study. Int J

Hydrogen Energy 2024;57:1197–207. https://doi.org/10.1016/J.IJHYDENE.2024.01.122.
[5] Viteri JP, Viteri S, Alvarez-Vasco C, Henao F. A systematic review on green hydrogen for off-grid communities –technologies, advantages, and limitations. Int J Hydrogen Energy 2023;48(52):19751–71. https://doi.org/10.1016/J.IJHYDENE.2023.02.078.
[6] Mérida García A, Gallagher J, Rodríguez Díaz JA, McNabola A. An economic and environmental optimization model for sizing a hybrid renewable energy and battery storage system in off-grid farms. Renew Energy 2024;220:119588. https://doi.org/10.1016/J.RENENE.2023.119588.
[7] Jansen G, Dehouche Z, Corrigan H. Cost-effective sizing of a hybrid Regenerative Hydrogen Fuel Cell energy storage system for remote & off-grid telecom towers. Int J Hydrogen Energy 2021;46(35):18153–66. https://doi.org/10.1016/J.IJHYDENE.2021.02.205.
[8] Mokhtara C, Negrou B, Bouferrouk A, Yao Y, Settou N, Ramadan M. Integrated supply–demand energy management for optimal design of off-grid hybrid renewable energy systems for residential electrification in arid climates. Energy Convers Manag 2020;221:113192. https://doi.org/10.1016/J.ENCONMAN.2020.113192.
[9] Ghorbani N, Kasaeian A, Toopshekan A, Bahrami L, Maghami A. Optimizing a hybrid wind-PV-battery system using GA-PSO and MOPSO for reducing cost and increasing reliability. Energy 2018;154:581–91. https://doi.org/10.1016/J.ENERGY.2017.12.057.
[10] Babatunde OM, Munda JL, Hamam Y. Hybridized off-grid fuel cell/wind/solar PV/battery for energy generation in a small household: a multi-criteria perspective. Int J Hydrogen Energy 2022;47(10):6437–52. https://doi.org/10.1016/J.IJHYDENE.2021.12.018.
[11] Ayodele TR, Mosetlhe TC, Yusuff AA, Ogunjuyigbe ASO. Off-grid hybrid renewable energy system with hydrogen storage for South African rural community health clinic. Int J Hydrogen Energy 2021;46(38):19871–85. https://doi.org/10.1016/J.IJHYDENE.2021.03.140.
[12] Zhao G, Nielsen ER, Troncoso E, Hyde K, Romeo JS, Diderich M. Life cycle cost analysis: a case study of hydrogen energy application on the Orkney Islands. Int J Hydrogen Energy 2019;44(19):9517–28. https://doi.org/10.1016/J.IJHYDENE.2018.08.015.
[13] REMOTE project – remote euproject. https://www.remote-euproject.eu/. [Accessed 7 June 2024].
[14] Green Hysland - Deployment of a H2 Ecosystem on the Island of Mallorca - https://greenhysland.eu/(accessed June 7, 2024).
[15] Clean energy vision to clean energy action | Clean energy for EU islands. https://clean-energy-islands.ec.europa.eu/. [Accessed 14 June 2024].
[16] Exploring hydrogen's potential in island communities: webinar highlights | clean energy for EU islands. https://clean-energy-islands.ec.europa.eu/news/exploring-hydrogens-potential-island-communities-webinar-highlights. [Accessed 14 June 2024].
[17] Why the Canary Islands are The for Pioneering Hydrogen. https://h2-heat.eu/blog/this-is-why-the-canary-islands-are-the-best-option-for-pioneering-hydrogen-projects-in-healthcare/(accessed June 14, 2024).
[18] The SEAFUEL project celebrates the arrival of the first Hydrogen Refueling Station to Tenerife, the first one in the Canary Islands – seafuel. https://www.seafuel.eu/the-seafuel-project-celebrates-the-arrival-of-the-first-hydrogen-refueling-station-to-tenerife-the-first-one-in-the-canary-islands/. [Accessed 14 June 2024].
[19] Big hit. https://www.bighit.eu/. [Accessed 14 June 2024].
[20] Decentralised energy supply with h2 and fuel cells on Thai islands (AHK Thailand) - NOW GmbH. https://www.now-gmbh.de/en/projectfinder/decentralised-energy-supply-with-h2-and-fuel-cells-on-thai-islands-ahk-thailand/. [Accessed 14 June 2024].
[21] Marocco P, Novo R, Lanzini A, Mattiazzo G, Santarelli M. Towards 100% renewable energy systems: the role of hydrogen and batteries. J Energy Storage 2023;57. https://doi.org/10.1016/J.EST.2022.106306.
[22] Marocco P, Ferrero D, Lanzini A, Santarelli M. Optimal design of stand-alone solutions based on RES + hydrogen storage feeding off-grid communities. Energy Convers Manag 2021;238. https://doi.org/10.1016/J.ENCONMAN.2021.114147.
[23] Nagasawa K, Miyazaki T, Iino Y, Hayashi Y, Shoji T, Yoshinaga J. Backup generator output control method of off-grid system based on renewable energy in remote island. In: Proceedings – 2020 international conference on smart grids and energy systems, *SGES 2020*; 2020. p. 169–74. https://doi.org/10.1109/SGES51519.2020.00037.
[24] Fukaume S, Nagasaki Y, Tsuda M. Stable power supply of an independent power source for a remote island using a Hybrid Energy Storage System composed of electric and hydrogen energy storage systems. Int J Hydrogen Energy 2022;47(29):13887–99. https://doi.org/10.1016/J.IJHYDENE.2022.02.142.
[25] Gracia L, Casero P, Bourasseau C, Chabert A. Use of hydrogen in off-grid locations, a techno-economic assessment. Energies 2018;11(11). https://doi.org/10.3390/EN11113141.
[26] Zhang X, Wei QS, Oh BS. Cost analysis of off-grid renewable hybrid power generation system on Ui Island, South Korea. Int J Hydrogen Energy 2022;47(27):13199–212. https://doi.org/10.1016/J.IJHYDENE.2022.01.150.
[27] Kalinci Y, Hepbasli A, Dincer I. Techno-economic analysis of a stand-alone hybrid renewable energy system with hydrogen production and storage options. Int J Hydrogen Energy 2015;40(24):7652–64. https://doi.org/10.1016/J.IJHYDENE.2014.10.147.
[28] Marczinkowski HM, Østergaard PA. Residential versus communal combination of photovoltaic and battery in smart energy systems. Energy 2018;152:466–75. https://doi.org/10.1016/J.ENERGY.2018.03.153.
[29] Dawood F, Shafiullah GM, Anda M. Stand-alone microgrid with 100% renewable energy: a case study with hybrid solar PV-Battery-Hydrogen. Sustainability 2020;12(5):2047. https://doi.org/10.3390/SU12052047. 2020, Vol. 12, Page 2047.
[30] Khiareddine A, ben Salah C, Rekioua D, Mimouni MF. Sizing methodology for hybrid photovoltaic/wind/hydrogen/battery integrated to energy management strategy for pumping system. Energy 2018;153:743–62. https://doi.org/10.1016/J.ENERGY.2018.04.073.
[31] Castañeda M, Cano A, Jurado F, Sánchez H, Fernández LM. Sizing optimization, dynamic modeling and energy management strategies of a stand-alone PV/hydrogen/battery-based hybrid system. Int J Hydrogen Energy 2013;38(10):3830–45. https://doi.org/10.1016/J.IJHYDENE.2013.01.080.
[32] Nordin ND, Rahman HA. Comparison of optimum design, sizing, and economic analysis of standalone photovoltaic/battery without and with hydrogen production systems. Renew Energy 2019;141:107–23. https://doi.org/10.1016/J.RENENE.2019.03.090.
[33] Zhang W, Maleki A, Rosen MA, Liu J. Optimization with a simulated annealing algorithm of a hybrid system for renewable energy including battery and hydrogen storage. Energy 2018;163:191–207. https://doi.org/10.1016/J.ENERGY.2018.08.112.
[34] Mulenga E, Kabanshi A, Mupeta H, Ndiaye M, Nyirenda E, Mulenga K. Techno-economic analysis of off-grid PV-Diesel power generation system for rural electrification: a case study of Chilubi district in Zambia. Renew Energy 2023;203:601–11. https://doi.org/10.1016/j.renene.2022.12.112.
[35] Haghighat Mamaghani A, Avella Escandon SA, Najafi B, Shirazi A, Rinaldi F. Techno-economic feasibility of photovoltaic, wind, diesel and hybrid electrification systems for off-grid rural electrification in Colombia. Renew Energy 2016;97:293–305. https://doi.org/10.1016/J.RENENE.2016.05.086.
[36] Das BK, Alotaibi MA, Das P, Islam MS, Das SK, Hossain A. Feasibility and techno-economic analysis of stand-alone and grid-connected PV/Wind/Diesel/Batt hybrid energy system: a case study. Energy Strategy Rev 2021;37:2211–467. https://doi.org/10.1016/j.esr.2021.100673.
[37] Ameri C, Ngouleu W, Wenceslas Koholé Y, Cyrille F, Fohagui V, Tchuen G. Optimal sizing and techno-enviro-economic evaluation of a hybrid photovoltaic/wind/diesel system with battery and fuel cell storage devices under different climatic conditions in Cameroon. J Clean Prod 2023;423:138753. https://doi.org/10.1016/j.jclepro.2023.138753.
[38] Trapani D, Marocco P, Ferrero D, Lindberg KB, Sundseth K, Santarelli M. The potential of hydrogen-battery storage systems for a sustainable renewable-based electrification of remote islands in Norway. J Energy Storage 2024;75:109482. https://doi.org/10.1016/J.EST.2023.109482.
[39] Hasan T, Emami K, Shah R, Hassan NMS, Belokoskov V, Ly M. Techno-economic assessment of a hydrogen-based islanded microgrid in north-east. Energy Rep 2023;9:3380–96. https://doi.org/10.1016/J.EGYR.2023.02.019.
[40] Baghaee HR, Mirsalim M, Gharehpetian GB, Talebi HA. Reliability/cost-based multi-objective Pareto optimal design of stand-alone wind/PV/FC generation microgrid system. Energy 2016;115:1022–41. https://doi.org/10.1016/J.ENERGY.2016.09.007.
[41] Shiva Kumar S, Lim H. An overview of water electrolysis technologies for green hydrogen production. Energy Rep 2022;8:13793–813. https://doi.org/10.1016/J.EGYR.2022.10.127.
[42] Ge L, Zhang B, Huang W, Li Y, Hou L, Xiao J, Mao Z, Li X. A review of hydrogen generation, storage, and applications in power system. J Energy Storage 2024;75:109307. https://doi.org/10.1016/J.EST.2023.109307.
[43] Mori M, Gutiérrez M, Casero P. Micro-grid design and life-cycle assessment of a mountain hut's stand-alone energy system with hydrogen used for seasonal storage. Int J Hydrogen Energy 2021;46(57):29706–23. https://doi.org/10.1016/J.IJHYDENE.2020.11.155.
[44] Chamout Mhd W, Perl A, Hengeveld EJ, Aué J. Simulation and analysis of hybrid hydrogen-battery renewable energy storage for off-electric-grid Dutch household system. Int J Hydrogen Energy 2024;70:170–82. https://doi.org/10.1016/J.IJHYDENE.2024.05.106.
[45] Li JQ, Li JC, Wang XY, Xu H, Kwon JT. A theoretical study on the hydrogen filling process of the on-board storage cylinder in hydrogen refueling station. Results in Engineering 2023;18:101168. https://doi.org/10.1016/J.RINENG.2023.101168.
[46] Abdin Z, Khalilpour K, Catchpole K. Projecting the levelized cost of large scale hydrogen storage for stationary applications. Energy Convers Manag 2022;270:116241. https://doi.org/10.1016/J.ENCONMAN.2022.116241.
[47] Ozsari I. Trend analysis and evaluation of hydrogen energy and hydrogen storage research. Energy Storage 2023;5(6):e471. https://doi.org/10.1002/EST2.471.
[48] Deng Z, Jiang Y. Optimal sizing of wind-hydrogen system considering hydrogen demand and trading modes. Int J Hydrogen Energy 2020;45(20):11527–37. https://doi.org/10.1016/J.IJHYDENE.2020.02.089.
[49] Sun K, Chen X, Maleki Dastjerdi S, Yang Q. Dynamic simulation of hydrogen-based off-grid zero energy buildings with hydrogen storage considering Fanger model thermal comfort. Int J Hydrogen Energy 2022;47(62):26435–57. https://doi.org/10.1016/J.IJHYDENE.2022.03.248.
[50] Jin L, Rossi M, Monforti Ferrario A, Alberizzi JC, Renzi M, Comodi G. Integration of battery and hydrogen energy storage systems with small-scale hydropower plants in off-grid local energy communities. Energy Convers Manag 2023;286:117019. https://doi.org/10.1016/J.ENCONMAN.2023.117019.
[51] Koholé YW, Wankouo Ngouleu CA, Fohagui FCV, Tchuen G. A comprehensive comparison of battery, hydrogen, pumped-hydro and thermal energy storage technologies for hybrid renewable energy systems integration. J Energy Storage 2024;93:112299. https://doi.org/10.1016/J.EST.2024.112299.

[52] Petrollese M, Concas G, Lonis F, Cocco D. Techno-economic assessment of green hydrogen valley providing multiple end-users. Int J Hydrogen Energy 2022;47(57):24121–35. https://doi.org/10.1016/J.IJHYDENE.2022.04.210.
[53] Kilic M, Altun AF. Dynamic modelling and multi-objective optimization of off-grid hybrid energy systems by using battery or hydrogen storage for different climates. Int J Hydrogen Energy 2022;48:22834–54. https://doi.org/10.1016/j.ijhydene.2022.12.103.
[54] He Y, Guo S, Dong P, Wang C, Huang J, Zhou J. Techno-economic comparison of different hybrid energy storage systems for off-grid renewable energy applications based on a novel probabilistic reliability index. Appl Energy 2022;328:120225. https://doi.org/10.1016/J.APENERGY.2022.120225.
[55] Zhang C, Wu J, Long C, Cheng M. Review of existing peer-to-peer energy trading projects. Energy Proc 2017;105:2563–8. https://doi.org/10.1016/J.EGYPRO.2017.03.737.
[56] Song Y, Xu L, Li J, Taherian H, Zhang Y, Liu D, Li Z, Hou G. Multi-objective optimization and long-term performance evaluation of a hybrid solar-hydrogen energy system with retired electric vehicle batteries for off-grid power and heat supply. Int J Hydrogen Energy 2024;62:867–82. https://doi.org/10.1016/J.IJHYDENE.2024.03.105.
[57] Yang Y, Wu Z, Yao J, Guo T, Yang F, Zhang Z, Ren J, Jiang L, Li B. An overview of application-oriented multifunctional large-scale stationary battery and hydrogen hybrid energy storage system. Energy Rev 2024;3(2):100068. https://doi.org/10.1016/J.ENREV.2024.100068.
[58] Yilanci A, Dincer I, Ozturk HK. A review on solar-hydrogen/fuel cell hybrid energy systems for stationary applications. Prog Energy Combust Sci 2009;35(3):231–44. https://doi.org/10.1016/J.PECS.2008.07.004.
[59] Ghirardi E, Brumana G, Franchini G, Aristolao N, Vedovati G. The role of hydrogen storage and electric vehicles in grid-isolated hybrid energy system with high penetration of renewable. Energy Convers Manag 2024;302:118154. https://doi.org/10.1016/J.ENCONMAN.2024.118154.
[60] Scamman D, Newborough M, Bustamante H. Hybrid hydrogen-battery systems for renewable off-grid telecom power. Int J Hydrogen Energy 2015;40(40):13876–87. https://doi.org/10.1016/J.IJHYDENE.2015.08.071.
[61] Martínez de León C, Ríos C, Molina P, Brey JJ. Levelized cost of storage (LCOS) for a hydrogen system. Int J Hydrogen Energy 2024;52:1274–84. https://doi.org/10.1016/J.IJHYDENE.2023.07.239.
[62] Rabiee A, Keane A, Soroudi A. Green hydrogen: a new flexibility source for security constrained scheduling of power systems with renewable energies. Int J Hydrogen Energy 2021;46(37):19270–84. https://doi.org/10.1016/J.IJHYDENE.2021.03.080.
[63] Khakimov R, Moskvin A, Zhdaneev O. Hydrogen as a key technology for long-term & seasonal energy storage applications. Int J Hydrogen Energy 2024;68:374–81. https://doi.org/10.1016/J.IJHYDENE.2024.04.066.
[64] Hosseinalizadeh R, Shakouri G H, Amalnick MS, Taghipour P. Economic sizing of a hybrid (PV–WT–FC) renewable energy system (HRES) for stand-alone usages by an optimization-simulation model: case study of Iran. Renew Sustain Energy Rev 2016;54:139–50. https://doi.org/10.1016/J.RSER.2015.09.046.
[65] Alonso AM, Costa D, Messagie M, Coosemans T. Techno-economic assessment on hybrid energy storage systems comprising hydrogen and batteries: a case study in Belgium. Int J Hydrogen Energy 2024;52:1124–35. https://doi.org/10.1016/J.IJHYDENE.2023.06.282.
[66] Guinot B, Champel B, Montignac F, Lemaire E, Vannucci D, Sailler S, Bultel Y. Techno-economic study of a PV-hydrogen-battery hybrid system for off-grid power supply: impact of performances' ageing on optimal system sizing and competitiveness. Int J Hydrogen Energy 2015;40(1):623–32. https://doi.org/10.1016/J.IJHYDENE.2014.11.007.
[67] Ahmad T, Zhang H, Yan B. A review on renewable energy and electricity requirement forecasting models for smart grid and buildings. Sustain Cities Soc 2020;55:102052. https://doi.org/10.1016/J.SCS.2020.102052.
[68] Zahedi A, Al-bonsrulah HAZ, Tafavogh M. Conceptual design and simulation of a stand-alone Wind/PEM fuel Cell/Hydrogen storage energy system for off-grid regions, a case study in Kuhin, Iran. Sustain Energy Technol Assessments 2023;57:103142. https://doi.org/10.1016/J.SETA.2023.103142.
[69] Bharatee A, Ray PK, Ghosh A. Power distribution technique and small-signal modeling of grid-integrated solar PV system with hybrid energy storage systems. J Energy Storage 2023;73:109316. https://doi.org/10.1016/J.EST.2023.109316.
[70] International Renewal Energy Agency I. Transforming small-island power systems technical planning studies for the integration of variable renewables. 2018. Abu Dhabi ISBN 978 – 92 – 9260 – 074 – 7.
[71] Meteotest Meteonorm Software—Worldwide Irradiation Data. https://meteonorm.com/en/(accessed May 12, 2022).
[72] Sunerg solar PHOTOVOLTAIC MODULE X-CLASSIC. https://www.sunergsolar.com/en/products/photovoltaic/photovoltaic-module/x-classic_55.html. [Accessed 20 October 2022].
[73] Duffie JA, Beckman WA. Solar engineering of thermal processes. fourth ed. 2013. https://doi.org/10.1002/9781118671603. Solar Engineering of Thermal Processes: Fourth Edition.
[74] AEM Electrolyser – Low-Cost Green Hydrogen – Enapter n.d. https://www.enapter.com/aem-electrolysers/aem-electrolyser-el-4/(accessed May 8, 2023).
[75] An L, Zhao TS, Chai ZH, Tan P, Zeng L. Mathematical modeling of an anion-exchange membrane water electrolyzer for hydrogen production. Int J Hydrogen Energy 2014;39(35):19869–76. https://doi.org/10.1016/J.IJHYDENE.2014.10.025.
[76] Gul E, Baldinelli G, Farooqui A, Bartocci P, Shamim T. AEM-electrolyzer based hydrogen integrated renewable energy system optimisation model for distributed communities. Energy Convers Manag 2023;285:117025. https://doi.org/10.1016/J.ENCONMAN.2023.117025.
[77] Omran A, Lucchesi A, Smith D, Alaswad A, Amiri A, Wilberforce T, Sodré JR, Olabi AG. Mathematical model of a proton-exchange membrane (PEM) fuel cell. International Journal of Thermofluids 2021;11:100110. https://doi.org/10.1016/J.IJFT.2021.100110.
[78] Spiegel C. PEM fuel cell modeling and simulation using matlab. PEM Fuel Cell Modeling and Simulation Using Matlab 2008:1–443. https://doi.org/10.1016/B978-0-12-374259-9.X5001-0.
[79] Serra F, Lucariello M, Petrollese M, Cau G. Optimal integration of hydrogen-based energy storage systems in photovoltaic microgrids: a techno-economic assessment. https://doi.org/10.3390/en13164149; 2020.
[80] Pereira Micena R, Llerena-Pizarro OR, Miguel de Souza T, Luz Silveira J. Solar-powered hydrogen refueling stations: a techno-economic analysis. https://doi.org/10.1016/j.ijhydene.2019.11.092; 2019.